Journal of Colloid and Interface Science 407 (2013) 450–456

Contents lists available at SciVerse ScienceDirect

Journal of Colloid and Interface Science

www.elsevier.com/locate/jcis

Biosorption of phenol onto bionanoparticles from *Spirulina* sp. LEB 18

G.L. Dotto *, J.O. Gonçalves, T.R.S. Cadaval Jr., L.A.A. Pinto

Unit Operation Laboratory, School of Chemistry and Food, Federal University of Rio Grande – FURG, 475 Engenheiro Alfredo Huch Street, 96203-900 Rio Grande, RS, Brazil

ARTICLE INFO

Article history:
Received 1 May 2013
Accepted 14 June 2013
Available online 27 June 2013

Keywords:
Biosorption
Equilibrium isotherms
Phenol
Thermodynamics

ABSTRACT

The biosorption of phenol onto bionanoparticles from *Spirulina* sp. LEB 18 was studied. Firstly, the bionanoparticles were prepared from *Spirulina* sp. strain LEB 18 and characterized. After, response surface methodology was employed to optimize the biosorption process as a function of pH (3.2–8.8) and bionanoparticles dosage (0.15–1.85 g L^{-1}). Finally, equilibrium and thermodynamic studies were performed at different temperatures (298–328 K). The bionanoparticles presented hydrodynamic diameter of 232 ± 3 nm and polydispersity index of 0.150. It was found that the more adequate condition for the phenol biosorption was pH of 6.0 and bionanoparticles dosage of 1.85 g L^{-1}. The Langmuir model presented satisfactory fit with the equilibrium experimental data. The maximum biosorption capacity was 159.33 mg g^{-1}, obtained at 298 K. The thermodynamic parameters showed that the biosorption was a spontaneous, favorable and exothermic process. Based on these results, it can be affirmed that the bionanoparticles are an alternative, renewable and eco-friendly biosorbent to removal phenol from aqueous solutions.

1. Introduction

World oil demand is expected to rise to 107 million barrels per day over the next two decades, and oil will account for 32% of the world's energy supply by 2030 [1]. As consequence, the generation of oil industry effluents will increase considerably. According to Coelho et al. [2], the volume of petroleum refinery effluents generated during processing is 0.4–1.6 times the amount of the crude oil processed [2]. These effluents contain a series of toxic organic compounds, which are harmful to the environment and human health [3]. Among these compounds, phenol is generally considered the most hazardous organic pollutant due its high toxicity even at low concentrations [4], and is registered as priority pollutant by the US Environmental Protection Agency (USEPA) [5]. Thus, the development of technologies for phenol removal from oil effluents, in order to minimize the environmental impacts is an important research field [1–4,6].

Some technologies have been used to removal phenol from oil effluents, such as, extraction, distillation, membrane separation [6], adsorption [3,7] and advanced oxidation processes [1,2,8]. Due to its ease of operation and high efficiency, adsorption has gained special attention in the recent literature [3,4,7,9–12]. However, its use is limited by the obtention and regeneration costs of activated carbon, which is, the most used adsorbent [3]. Alternatively, biosorption can be employed to remove phenol from aqueous solutions, because it combines the advantages of adsorption with the use of natural, low-cost and renewable biosorbents [13]. In this context, many biosorbents have been studied, for example, *Aspergillus niger* [14], fungal mycelia [15], marine seaweeds [16], *Funalia trogii* [17], chitosan [18], *Phanerochaete chrysosporium* [19] and others [3]. In spite of this, studies about the applicability of *Spirulina* sp. as biosorbent to remove phenol from aqueous solutions are not found in the literature.

Spirulina sp. has been successfully employed to remove pollutants, such as heavy metals [20–23], food dyes and textile dyes [24–29] from aqueous solutions due the following characteristics: availability in large quantities, largely cultivated worldwide, contain a variety of functional groups (carboxyl, hydroxyl, sulfate, phosphate and others), low-cost, eco-friendly and renewable [20–30]. Recently, our research group has produced nanoparticles from *Spirulina platensis* strain LEB 52 [23,24,26,27]. We verified its good potentiality for the biosorption of Cr (VI) [23] and dyes [24,26,27]. So, to extend the applicability of *Spirulina* sp. as biosorbent, it is interesting to verify the behavior of other strains, and also the possibility to removal others pollutants like phenol.

This work aimed to verify the biosorption potential of bionanoparticles from *Spirulina* sp. LEB 18 for the removal phenol from aqueous solutions. The bionanoparticles were prepared from *Spirulina* sp. strain LEB 18 and characterized by dynamic light scattering (DLS) and Fourier transform infrared analysis (FTIR-ATR).

* Corresponding author. Fax: +55 53 3233 8745.
E-mail addresses: guilherme_dotto@yahoo.com.br (G.L. Dotto), janaina_sde@hotmail.com (J.O. Gonçalves), titoeq@gmail.com (T.R.S. Cadaval Jr.), dqmpinto@furg.br (L.A.A. Pinto).

0021-9797/$ - see front matter © 2013 Elsevier Inc. All rights reserved.
http://dx.doi.org/10.1016/j.jcis.2013.06.044

The effects of pH (3.2–8.8) and bionanoparticles dosage (0.15–1.85 g L^{-1}) on the biosorption were evaluated by response surface methodology. Equilibrium studies were performed at different temperatures (298–328 K) using the Langmuir and Freundlich isotherm models. The Gibbs free energy change (ΔG^0), enthalpy change (ΔH^0) and entropy change (ΔS^0) were estimated to elucidate the biosorption thermodynamic behavior.

2. Materials and methods

2.1. Production of Spirulina sp. LEB 18 biomass

The culture was inoculated in 1 L photobioreactor with initial *Spirulina* sp. concentration of 0.15 g L^{-1}. The bioreactor was maintained at 30 °C in a growth chamber under a 12 h light/dark photo period and an incident light intensity of 32.5 μmol m^{-2} s^{-1}, provided by appropriate numbers of 40 W day light type fluorescent tubes. Strain LEB 18 was cultivated in 20% Zarrouk medium, diluted with sterilized Mangueira Lagoon water. Each bioreactor run lasted 38 days during which time the cultures were agitated and aerated with 20 L h^{-1} air supplied by diaphragm pumps [31]. Samples were aseptically collected every 24 h and the biomass concentration determined by optical density at 670 nm (Quimis, Q108, Brazil) [32]. At the end of cultivation, the biomass was recovered by filtration and pressed to recover the biomass with a moisture content of 76% (wet basis) [32].

The wet biomass (cylindrical pellet form with a diameter of 3 mm) was dried in perforated trays using perpendicular air flow. The drying conditions were: air temperature 60 °C, air velocity 1.5 m s^{-1}, relative humidity between 7% and 10%, load in tray 4 kg m^{-2} [33]. The dried biomass was ground by using a mill (Wiley Mill Standard, No. 03, USA) and was sieved until the discrete particle size ranged from 68 to 75 μm.

2.2. Preparation and characterization of the bionanoparticles

The suspension of bionanoparticles was obtained from dried biomass of *Spirulina* sp. strain LEB 18, according to the procedure developed in our recent published works [23,24,26]. The sieved biomass (concentrations in the range from 0.30 to 3.70 g L^{-1}) was added in distilled water and the pH was adjusted (3.2–8.8) by buffer disodium phosphate/citric acid solution (0.1 mol L^{-1}). After, the suspension was agitated (Dremel, 1100-01, Brazil) at 10,000 rpm for 20 min.

The size distribution, hydrodynamic diameter, polydispersity index and autocorrelation function of the bionanoparticles were evaluated in suspension by dynamic light scattering (DLS) [34]. The dynamic light scattering equipment was constituted by a laser (Spectra-physics, 127, USA) coupled to a goniometer (Brookheaven, BI-200M, USA) and a digital correlator (Brookheaven, BI-9000AT, USA). The identification of the functional groups was carried out using infrared analysis with attenuated total reflectance (FTIR-ATR) (Prestige 21, the 210045, Japan) [24].

2.3. Biosorption experiments

Firstly, stock solutions were prepared (1.0 g L^{-1}) by diluting solid phenol (94.11 g mol^{-1}, purity of 99.9%) (Vetec, Brazil) in distilled water [17]. All subsequent tests were realized by diluting this solution. After, biosorption tests were carried out in two steps: response surface methodology (RSM) experiments and equilibrium experiments. For the RSM experiments, the initial phenol concentration was 200 mg L^{-1} and the effects of pH (3.2–8.8) and bionanoparticles dosage (0.15–1.85 g L^{-1}) were evaluated. The flasks were agitated at 100 rpm and 298 K using thermostated type Wagner agitator (Fanem, 315 SE, Brazil) for 24 h. For the equilibrium experiments, pH and bionanoparticles dosage were fixed (according RSM results) and the initial phenol concentration ranged from 50 to 500 mg L^{-1}. Flasks were agitated at 100 rpm (Fanem, 315 SE, Brazil) under different temperatures (298–328 K) until equilibrium. The solutions were centrifuged (Centribio, 80-2B, Brazil) at 4000 rpm for 20 min and the phenol concentration was determined by spectrophotometer (Shimadzu, UV-240, Japan) at 270 nm [17]. All experiments were carried out in replicate (three times for each experiment) and blanks were performed. The phenol percentage removal (R) and the equilibrium biosorption capacity (q_e) were determined by Eqs. (1) and (2), respectively:

$$R = \frac{C_0 - C_f}{C_0} 100 \quad (1)$$

$$q_e = \frac{C_0 - C_e}{m} V \quad (2)$$

where C_0 is the initial phenol concentration in liquid phase (mg L^{-1}), C_f is the final phenol concentration in liquid phase (mg L^{-1}), C_e is the equilibrium phenol concentration in liquid phase (mg L^{-1}), m is amount of bionanoparticles (g), and V is the volume of solution (L).

2.4. Response surface methodology (RSM)

It is know in the literature, that the phenol biosorption is affected by various factors, such as pH, temperature, initial concentration, biosorbent dosage, stirring rate and contact time [1,6,13–15,17–19]. In this context, response surface methodology (RSM) is a good way to verify the influence of these factors on the phenol biosorption [20,23,25,35]. In this research, RSM was employed to optimize the phenol biosorption as a function of pH and bionanoparticles dosage. The levels and factors of a central composite design (2^2 with three central and four axial points) were selected by preliminary tests and literature [1,3,4,7–19] and are showed in Table 1.

The phenol percentage removal (R) was represented as function of independent variables according to [35]:

$$R = a + \sum_{i=1}^{n} b_i x_i + \sum_{i=1}^{n} b_{ii} x_i^2 + \sum_{i=1}^{n-1} \sum_{j=i+1}^{n} b_{ij} x_i x_j \quad (3)$$

where R is the predicted response, "a" the constant coefficient, "b_i" the linear coefficients, "b_{ij}" the interaction coefficients, "b_{ii}" the quadratic coefficients, "x_i" and "x_j" are the coded values of the variables.

The results were analyzed using Statistic version 7 (StatSoft Inc., USA) software. The second order model (Eq. (3)) was evaluated by Fischer's test, and the proportion of variance explained by the

Table 1
Factors, levels and experimental results for the phenol percentage removal (R) according to the central composite design.

pH	Bionanoparticles dosage (g L^{-1})	R (%)[a]
8.0 (+1)	1.60 (+1)	40.8 ± 1.1
4.0 (−1)	1.60 (+1)	45.3 ± 0.2
8.0 (+1)	0.40 (−1)	20.9 ± 0.3
4.0 (−1)	0.40 (−1)	17.8 ± 0.2
6.0 (0)	1.00 (0)	38.2 ± 1.0
6.0 (0)	1.00 (0)	37.3 ± 1.2
6.0 (0)	1.00 (0)	37.7 ± 0.9
6.0 (0)	1.85 (+1.41)	51.5 ± 0.8
6.0 (0)	0.15 (−1.41)	9.8 ± 0.1
8.8 (+1.41)	1.00 (0)	14.6 ± 0.4
3.2 (−1.41)	1.00 (0)	18.6 ± 0.1

[a] Mean ± standard error (n = 3).

model was given by the multiple coefficient of determination, R^2. The significance level was 95% ($p < 0.05$), and the non-significant factors were excluded [23,25,35].

2.5. Isotherm models

Equilibrium isotherm curves were obtained at 298, 308, 318 and 328 K for the biosorption of phenol onto bionanoparticles. In order to fit these equilibrium biosorption curves, Freundlich and Langmuir isotherm models were applied. The Freundlich isotherm assumes that the biosorption occurs on a heterogeneous surface, and the amount that is biosorbed increases infinitely with an increase in concentration. The Freundlich isotherm is given by [36]:

$$q_e = k_F C_e^{1/n_F} \tag{4}$$

where k_F is the Freundlich constant (mg g^{-1})(mg L^{-1})$^{-1/nF}$ and $1/n_F$ is the heterogeneity factor.

The Langmuir isotherm model assumes a monolayer biosorption onto a homogeneous surface where the binding sites have equal affinity and energy. The Langmuir isotherm is given by [37]:

$$q_e = \frac{q_m k_L C_e}{1 + (k_L C_e)} \tag{5}$$

where q_m is the maximum biosorption capacity (mg g^{-1}) and k_L is the Langmuir constant (L mg^{-1}).

The equilibrium parameters were determined by the fit of the models with the experimental data through nonlinear regression. The calculations were carried out by the Quasi–Newton estimation method using the Statistic 7.0 software (Statsoft, USA) [38]. The fit quality was measured through determination coefficient (R^2), adjusted determination coefficient (R^2_{adj}) [38], average relative error (ARE), sum of squared errors (SSE) [39] and Akaike information criterion (AIC) [40], as showed in Eqs. (6), (7), (8), (9) and (10), respectively:

$$R^2 = \left(\frac{\sum_i^n (q_{i,\mathrm{exp}} - \bar{q}_{i,\mathrm{exp}})^2 - \sum_i^n (q_{i,\mathrm{exp}} - q_{i,\mathrm{model}})^2}{\sum_i^n (q_{i,\mathrm{exp}} - \bar{q}_{i,\mathrm{exp}})^2} \right) \tag{6}$$

$$R^2_{adj} = 1 - (1 - R^2) \cdot \left(\frac{n-1}{n-p} \right) \tag{7}$$

$$\mathrm{ARE} = \frac{100}{n} \sum_{i=1}^{n} \left| \frac{q_{i,\mathrm{model}} - q_{i,\mathrm{exp}}}{q_{i,\mathrm{exp}}} \right| \tag{8}$$

$$\mathrm{SSE} = \sum_{i=1}^{n} (q_{i,\mathrm{model}} - q_{i,\mathrm{exp}})^2 \tag{9}$$

$$\mathrm{AIC} = n \ln \left(\frac{\mathrm{SSE}}{n} \right) + 2p + \frac{2p(p+1)}{n-p-1} \tag{10}$$

where $q_{i,\mathrm{model}}$ is each value of q predicted by the fitted model, $q_{i,\mathrm{exp}}$ is each value of q measured experimentally, $\bar{q}_{i,\mathrm{exp}}$ is the average of q experimentally measured, n is the number of experimental points, and p is the number of parameters of the fitted model [38–40].

2.6. Thermodynamic parameters

The values of Gibbs free energy change (ΔG^0, kJ mol^{-1}), enthalpy change (ΔH^0, kJ mol^{-1}) and entropy change (ΔS^0, kJ mol^{-1} K^{-1}) were estimated from the best isotherm model according to [41,42]:

$$\Delta G^0 = -RT \ln(55.5 K_e) \tag{11}$$

$$\Delta G^0 = \Delta H^0 - T\Delta S^0 \tag{12}$$

$$\ln(55.5 K_e) = \frac{\Delta S^0}{R} - \frac{\Delta H^0}{RT} \tag{13}$$

where K_e is the thermodynamic equilibrium constant (L mol^{-1}), T is the temperature (K), R is the universal gas constant (8.31×10^{-3} - kJ mol^{-1} K^{-1}) and 55.5 is the number of moles of water per liter of solution. The K_e values were estimated from the parameters of the best fit isotherm model and the molecular weight phenol [26,41,42].

3. Results and discussion

3.1. Characteristics of bionanoparticles from Spirulina sp. LEB 18

The bionanoparticles from *Spirulina* sp. LEB 18 were characterized according its size distribution, hydrodynamic diameter, polydispersity index, autocorrelation function and functional groups. The size distribution and autocorrelation function are showed in Fig. 1a and b, respectively.

It was found in Fig. 1a that the bionanoparticles size ranged from 50 to 500 nm. The mean hydrodynamic diameter and polydispersity index (obtained by DLS) were 232 ± 3 nm and 0.150, respectively. The autocorrelation function (Fig. 1b) was unimodal. These results shows that the bionanoparticles from *Spirulina* sp. LEB 18 were stable, relatively monodisperse and presented a little variation in the size [23,24,26,27,34]. The nanoparticles from *S. platensis* LEB 52 obtained in our recent works [23,24] presented similar characteristics and were effective to remove Cr (VI) and dyes.

The functional groups of bionanoparticles from *Spirulina* sp. LEB 18 were identified by FTIR-ATR and the spectrum is presented in Fig. 2.

The major intense bands were observed at 3365, 3280, 2900, 1650, 1635, 1550, 1540, 1458, 1419, 1388, 1151, 1028, 950, 850 and 700 cm^{-1} (Fig. 2). The bands 3365 and 3280 cm^{-1} can be assigned to the O–H and N–H stretchings [24]. The asymmetric stretching of CH_2 can be observed at 2900 cm^{-1} [25]. The scissor

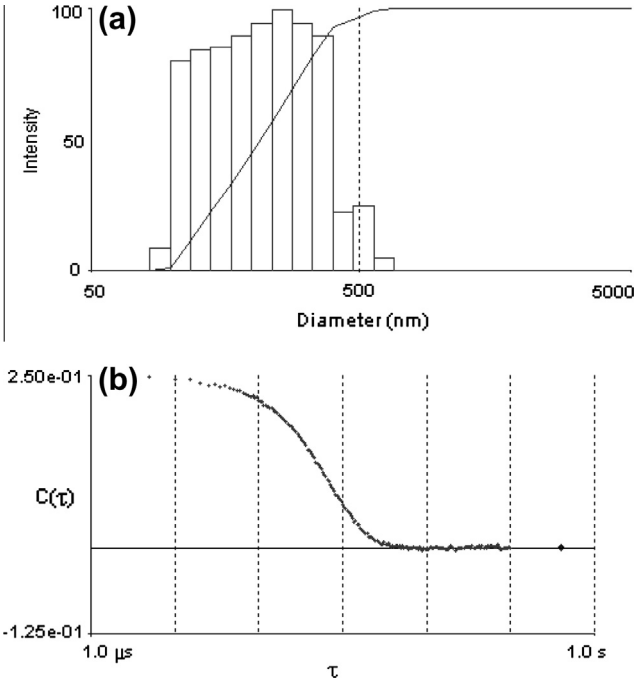

Fig. 1. Characteristics of bionanoparticles from *Spirulina* sp. LEB 18: (a) size distribution and (b) autocorrelation function.

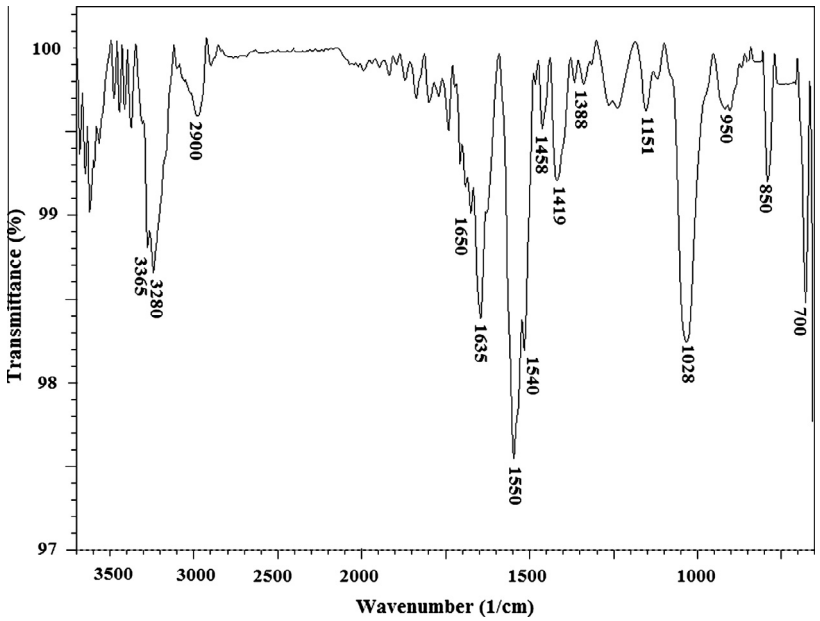

Fig. 2. FTIR-ATR spectrum of bionanoparticles from *Spirulina* sp. LEB 18.

Table 2
Analysis of variance (ANOVA) for the phenol percentage removal.[a]

Factor	Sum of square	Degree of freedom	Mean of square	*F*	*p*
pH (linear)	6.09	1	6.09	30.86	0.0309
pH (quadratic)	420.71	1	420.71	2132.14	0.0005
Dosage (linear)	1414.75	1	1414.75	7169.82	0.0001
Dosage (quadratic)	14.85	1	14.85	75.25	0.0130
pH by dosage	14.26	1	14.26	72.25	0.0135
Lack of fit	137.19	3	45.73	231.75	0.0043
Pure error	0.40	2	0.20		
Total	1998.32	10			

[a] $R^2 = 0.9611$.

bending of NH_2 group can be observed at 1650 and 1635 cm^{-1}. The interaction N–H bending with C–N stretching can be observed at 1550 and 1540 cm^{-1}. The bending of NH_4^+ was identified at 1458 cm^{-1} [24,25]. The band at 1419 cm^{-1} is relative to the C–N stretching of primary amide [28,29]. The aldehydes and ketones groups can be observed at 1388 and 1151 cm^{-1}, respectively [29]. The bands in the region of 700–1028 cm^{-1} could be attributed to –P–O, –S–O, and aromatic –CH stretching vibrations [20]. In summary, the FTIR-ATR spectrum showed that the bionanoparticles from *Spirulina* sp. LEB 18 have a variety of biomacromolecules and functional groups on the surface. The literature shows that these functional groups can be responsible for binding with copper [20], cadmium [21], chromium [23], synthetic dyes [24], food dyes [26,27] and textile dyes [29].

3.2. Biosorption optimization

The phenol biosorption onto bionanoparticles from *Spirulina* sp. LEB 18 was optimized by response surface methodology (RSM). A central composite design (2^2 with three central and four axial points) was employed to verify the effects of pH and bionanoparticles dosage on the phenol percentage removal (R). The RSM results are shown in Table 1. To verify the significance of pH and bionanoparticles dosage on the phenol percentage removal (R), analysis of variance (ANOVA) was applied to the experimental data and the results are shown in Table 2. It was found from the ANOVA (Table 2) that the linear and quadratic effects of pH and bionanoparticles dosage and also the interaction effect were significant ($p < 0.05$) in relation to the phenol percentage removal (R).

Thus, a statistical polynomial quadratic model was developed in order to represent the phenol percentage removal (R) as a function of pH (x_1) and bionanoparticles dosage (x_2), as demonstrated in

$$R = 37.7 - 0.87x_1 + 13.3x_2 - 8.7x_1^2 - 1.6x_2^2 - 1.9x_1x_2 \quad (14)$$

where x_1 and x_2 are the coded values of pH and bionanoparticles dosage, respectively.

The prediction and significance of the statistical model was evaluated by analysis of variance and Fischer's F test [35]. The high value of determination coefficient ($R^2 = 0.9611$) showed that the model was significant. The calculated F value ($F_{CALC} = 13.52$) was 2.67 times higher than standard F value ($F_{TAB} = 5.05$) showing that the model was predictive. The distribution of residues was random around zero, showing that the model was not biased. In this way, Eq. (14) was employed to generate the response surface which represents the percentage removal (R) as a function of pH and bionanoparticles dosage. The response surface for the phenol percentage removal as a function of pH and bionanoparticles dosage is presented in Fig. 3.

It was found in Fig. 3 that the phenol percentage removal (R) presented a parabolic dependence in relation to the pH with

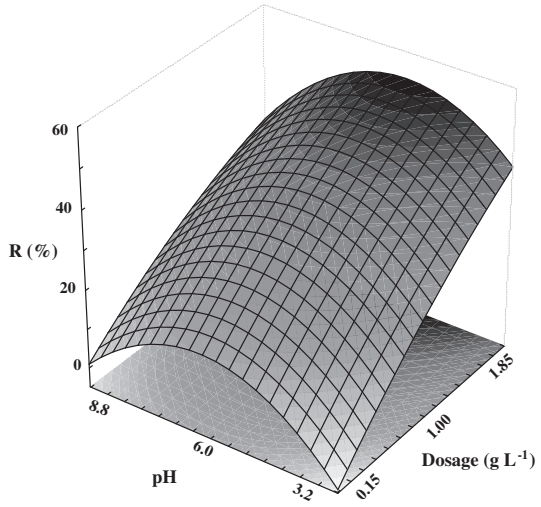

Fig. 3. Response surface for the phenol percentage removal as a function of pH and bionanoparticles dosage.

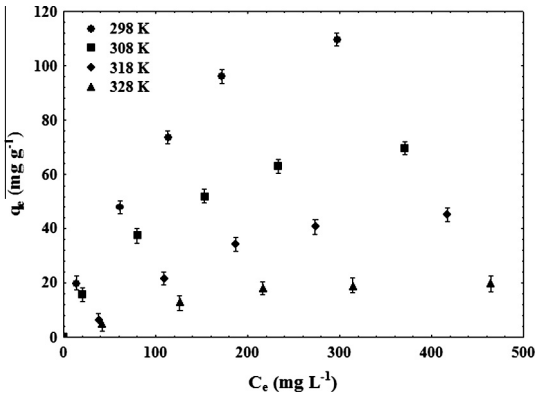

Fig. 4. Equilibrium curves for the phenol biosorption onto bionanoparticles from *Spirulina* sp. LEB 18.

maximum point at pH 6.0. This occurred because at low pH values (pH < 7.0), the bionanoparticles are positively charged [23–28] and the H^+ ion concentration in solution is high, therefore, competition between H^+ and phenol could occur, reducing the biosorbent–phenol interactions [43]. When the pH is increased to 6.0, the H^+ ion concentration in solution is lower, and the phenol access to the biosorption sites is facilitated, consequently, the percentage removal is higher. A new increase to 8.8 causes an increase in the electronic repulsion forces between the phenol molecules and the bionanoparticles surface, since that the bionanoparticles are negatively charged (pH > 7.0) [23–28] and phenol can dissociate to form phenolate anions [44]. As consequence, the percentage removal is reduced. Similar behavior was obtained by Li et al. [43] in the adsorption of phenol onto graphene. They obtained best results in the pH range from 4.0 to 6.6. Mubarik et al. [45] studied the phenol adsorption onto sheesham sawdust at the pH range from 2 to 10. They found that the adsorption increased with increase in pH up to 6.0, and decreased when pH was increased further.

Fig. 3 shows that an increase in the bionanoparticles dosage caused a strong increase in the phenol percentage removal, being the maximum values attained with 1.85 g L^{-1}. This occurred because high bionanoparticles dosage in the solution provides more available binding sites for the phenol biosorption. Bayramoglu et al. [17] studied the effect of biosorbent dosage (from 0.25 to 2.0 g L^{-1}) in the phenol biosorption onto *F. trogii* pellets and obtained similar results.

In the considered work range, the more adequate conditions for the phenol biosorption onto bionanoparticles from *Spirulina* sp. LEB 18 were obtained by determining the maximum point of response surface (Fig. 3). These conditions were pH of 6.0 and bionanoparticles dosage of 1.85 g L^{-1}. The phenol percentage removal (R) obtained under these conditions was 53.2%.

3.3. Equilibrium studies

The equilibrium curves were obtained at different temperatures (298, 308, 318 and 328 K) under the following fixed conditions: pH 6.0, bionanoparticles dosage of 1.85 g L^{-1} and initial phenol concentration from 50 to 500 mg L^{-1}. The equilibrium curves for the phenol biosorption onto bionanoparticles from *Spirulina* sp. LEB 18 are showed in Fig. 4.

Fig. 4 shows that the biosorption isotherms were characterized by an initial step with increase in biosorption capacity, indicating a great bionanoparticles–phenol affinity and numerous readily accessible sites [26,28]. The isotherms can be classified as type L [46], indicating that no strong competition exists between the phenol and the solvent to occupy the biosorption sites [11]. This corroborates with the high values of phenol percentage removal (R) obtained at pH 6.0 (Section 3.2). Podkoscielny and Nieszporek [11] obtained similar behavior in the adsorption of phenols from aqueous solutions. It was also observed from Fig. 4 that the phenol biosorption capacity increased with the temperature decrease, being the best results obtained at 298 K. This occurred, probably, because the temperature increase causes damages of the sites on the surface of *Spirulina* sp., and, consequently a decrease in the surface activity [13,26,28,29]. Al-Muhtaseb et al. [47], using poly (methyl methacrylate) as adsorbent, verified that the phenol adsorption capacity decreased from 35.08 to 23.53 mg g^{-1} with an increase in temperature from 298 to 328 K.

Freundlich and Langmuir isotherm models were used to fit the equilibrium experimental data for the phenol biosorption onto bionanoparticles from *Spirulina* sp. LEB 18, and the results are showed in Table 3. The higher values of determination coefficient ($R^2 > 0.98$), adjusted determination coefficient ($R^2_{adj} > 0.97$) and the lower values of average relative error (ARE < 10%), sum of squared errors (SSE < 61) and Akaike information criterion (AIC < 22) were observed for the Langmuir model (Table 3). This shows that the Langmuir model was the more adequate to represent the phenol biosorption onto bionanoparticles from *Spirulina*

Table 3
Equilibrium parameters for the phenol biosorption onto bionanoparticles from *Spirulina* sp. LEB 18.

Model	Temperature (K)			
	298	308	318	328
Freundlich				
k_F (mg g^{-1})(mg L^{-1})$^{-1/nF}$	6.33	5.07	1.26	1.35
$1/n_F$	0.51	0.45	0.60	0.45
R^2	0.9839	0.9860	0.9592	0.9431
R^2_{adj}	0.9798	0.9825	0.9490	0.9289
ARE (%)	7.87	7.60	19.42	15.19
SSE	148.85	52.15	69.96	18.98
AIC	27.267	20.974	22.737	14.909
Langmuir				
q_m (mg g^{-1})	159.33	90.74	76.87	26.85
k_L (L mg^{-1})	0.0078	0.0090	0.0037	0.0070
R^2	0.9935	0.9987	0.9843	0.9811
R^2_{adj}	0.9919	0.9984	0.9804	0.9764
ARE (%)	6.48	2.38	9.07	7.96
SSE	60.62	4.97	26.96	6.29
AIC	21.887	6.876	17.016	8.286

Table 4
Comparison of bionanoparticles from *Spirulina* sp. LEB 18 with other materials for phenol removal.

Sorbent material	Sorbent dosage ($g\ L^{-1}$)	pH	Temperature (K)	Adsorption capacity ($mg\ g^{-1}$)	Reference
Activated carbon from soybean straw	–	–	–	278.0	[7]
Date-pit activated carbon	4.0	8.0	298	262.3	[4]
Organobentonite	5.0	5.0	288	193.0	[48]
Bionanoparticles from *Spirulina* sp. LEB 18	1.85	6.0	298	159.33	This work
Funalia trogii pellets	0.25	8.0	298	147.0	[17]
Activated carbon from tea industry waste	2.0	6.0	298	142.9	[49]
Porous carbon from vinegar lees	5.0	–	298	112.36	[50]
Chitosan calcium alginate blended beads	4.0	7.0	298	108.69	[18]
Basic anion exchange resin	5.0	11.2	303	92.9	[12]
Graphene	0.5	6.3	333	53.19	[43]
Natural zeolites	2.0	4.0	298	34.5	[9]
White-rot fungus	0.3	6.0	295.5	13.5	[19]
Fungal mycelia	5.0	–	298	5.0	[15]

Table 5
Thermodynamic parameters for the phenol biosorption onto bionanoparticles from *Spirulina* sp. LEB 18.

Temperature (K)	K_e ($L\ mol^{-1}$)[a]	ΔG^0 ($kJ\ mol^{-1}$)[a]	ΔH^0 ($kJ\ mol^{-1}$)[a]	ΔS^0 ($kJ\ mol^{-1}\ K^{-1}$)[a]
298	116.9 ± 2.1	−21.7 ± 0.1	−54.5 ± 1.2	−0.11 ± 0.01
308	76.8 ± 0.7	−21.3 ± 0.1		
318	26.8 ± 1.5	−19.3 ± 0.1		
328	17.7 ± 0.3	−18.7 ± 0.1		

[a] Mean ± standard error.

sp. LEB 18 in all studied temperatures. The Langmuir model was the more adequate also in the phenol adsorption onto date-pit activated carbon [4], activated carbon prepared from soybean straw [7], basic anion exchange resin [12], *F. trogii* pellets [17] and chitosan–calcium alginate blended beads [18]. The q_m values increased with the temperature decrease (Table 3), confirming that the phenol biosorption was favored at lower temperatures.

In this work, the maximum biosorption capacity was 159.33 $mg\ g^{-1}$ obtained at 298 K (Table 3). This value can be compared with the literature, as demonstrated in Table 4. Table 4 shows that the bionanoparticles from *Spirulina* sp. LEB 18 showed good biosorption capacity for phenol. In this way, it can be affirmed that the bionanoparticles from *Spirulina* sp. LEB 18 are an alternative, renewable and eco-friendly biosorbent to removal phenol from aqueous solutions.

3.4. Biosorption thermodynamics

The biosorption thermodynamic study was realized through the estimation of thermodynamic equilibrium constant, Gibbs free energy change, enthalpy change and entropy change. The thermodynamic parameters for the phenol biosorption onto bionanoparticles from *Spirulina* sp. LEB 18 are showed in Table 5.

It was found in Table 5 that the K_e values increased with the temperature decrease, showing that the bionanoparticles–phenol affinity is higher at 298 K. The negative values of ΔG^0 indicate that the phenol biosorption onto bionanoparticles from *Spirulina* sp. LEB 18 was a spontaneous and favorable process at all the studied temperatures. The enthalpy changes (ΔH^0) indicate that biosorption followed an exothermic process (Table 5). In addition, the magnitude of enthalpy was consistent with physical interactions [51,52]. The negative ΔS^0 values indicate that randomness decreases at the solid–solution interface during the biosorption. Similar thermodynamic behavior was obtained by Yousef et al. [9] in the phenol adsorption on zeolites.

4. Conclusion

In this research, bionanoparticles were obtained from *Spirulina* sp. strain LEB 18, and its biosorption potential for the removal phenol from aqueous solutions was evaluated. The bionanoparticles were stable, monodisperse and presented hydrodynamic diameter of 232 ± 3 nm. Response surface methodology showed that the more adequate condition for the phenol biosorption was pH of 6.0 and bionanoparticles dosage of 1.85 $g\ L^{-1}$. In this condition, the phenol percentage removal was 53.2%. The equilibrium study demonstrated that the Langmuir model presented satisfactory fit with the experimental data, and the maximum biosorption capacity was 159.33 $mg\ g^{-1}$, obtained at 298 K. The thermodynamic parameters showed that the biosorption was a spontaneous, favorable and exothermic process. In summary, these results demonstrated that the bionanoparticles from *Spirulina* sp. LEB 18 are an alternative, renewable and eco-friendly biosorbent to removal phenol from aqueous solutions.

Acknowledgments

The authors would like to thank CAPES (Brazilian Agency for Improvement of Graduate Personnel), CNPq (National Council of Science and Technological Development) and REDE NANOFOTOBIOTEC for the financial support.

References

[1] B.H. Diya'uddeen, W.M.A.W. Daud, A.R. Abdul Aziz, Process Saf. Environ. Prot. 89 (2011) 95–105.
[2] A. Coelho, A.V. Castro, M. Dezotti, G.L. Sant'anna Jr., J. Hazard. Mater. 137 (2006) 178–184.
[3] S.H. Lin, R.S. Juang, J. Environ. Manage. 90 (2009) 1336–1349.
[4] M.H. El-Naas, S. Al-Zuhair, M.A. Alhaija, Chem. Eng. J. 162 (2010) 997–1005.
[5] USEPA, Technical Support Document for Water Quality Based Toxics Control, EPA/440/485032, United States Environmental Protection Agency, Washington, DC, USA, 1985.
[6] G. Busca, S. Berardinelli, C. Resini, L. Arrighi, J. Hazard. Mater. 160 (2008) 265–288.
[7] Q. Miao, Y. Tang, J. Xu, X. Liu, L. Xiao, Q. Chen, J. Taiwan Inst. Chem. Eng. 44 (2013) 458–465.
[8] S.N. Hussain, E.P.L. Roberts, H.M.A. Asghar, A.K. Campen, N.W. Brown, Electrochim. Acta 92 (2013) 20–30.
[9] R.I. Yousef, B. El-Eswed, A.H. Al-Muhtaseb, Chem. Eng. J. 171 (2011) 1143–1149.
[10] J.L. Figueiredo, N. Mahata, M.F.R. Pereira, M.J. Sanchez Montero, J. Montero, F. Salvador, J. Colloid Interface Sci. 357 (2011) 210–214.
[11] P. Podkoscielny, K. Nieszporek, J. Colloid Interface Sci. 354 (2011) 282–291.
[12] L. Zhu, Y. Deng, J. Zhang, J. Chen, J. Colloid Interface Sci. 364 (2011) 462–468.
[13] Z. Aksu, Proc. Biochem. 40 (2005) 997–1026.
[14] J.R. Rao, T. Viraraghavan, Bioresour. Technol. 85 (2002) 165–171.
[15] J. Wu, H.Q. Yu, Proc. Biochem. 41 (2006) 44–49.
[16] A.E. Navarro, R.F. Portales, M.R. Sun-Kou, B.P. Llanos, J. Hazard. Mater. 156 (2008) 405–411.

[17] G. Bayramoglu, I. Gursel, Y. Tunali, M.Y. Arica, Bioresour. Technol. 100 (2009) 2685–2691.
[18] S.K. Nadavala, K. Swayampakula, V.M. Boddu, K. Abburi, J. Hazard. Mater. 162 (2009) 482–489.
[19] V. Farkas, A. Felinger, A. Hegedusova, I. Dékány, T. Pernyeszi, Colloids Surf., B 103 (2013) 381–390.
[20] A. Çelekli, M. Yavuzatmac, H. Bozkurt, J. Hazard. Mater. 173 (2010) 123–129.
[21] L. Fang, C. Zhou, P. Cai, W. Chen, X. Rong, K. Dai, W. Liang, J. Gu, Q. Huang, J. Hazard. Mater. 190 (2011) 810–815.
[22] M.S. Rodrigues, L.S. Ferreira, J.C. Monteiro de Carvalho, A. Lodi, E. Finocchio, A. Converti, J. Hazard. Mater. 217 (218) (2012) 246–255.
[23] G.L. Dotto, T.R.S. Cadaval Jr., L.A.A. Pinto, J. Ind. Eng. Chem. 18 (2012) 1925–1930.
[24] G.L. Dotto, T.R.S. Cadaval Jr., L.A.A. Pinto, Proc. Biochem. 47 (2012) 1335–1343.
[25] G.L. Dotto, V.M. Esquerdo, M.L.G. Vieira, L.A.A. Pinto, Colloids Surf., B 91 (2012) 234–241.
[26] G.L. Dotto, E.C. Lima, L.A.A. Pinto, Bioresour. Technol. 103 (2012) 123–130.
[27] G.L. Dotto, L.A.A. Pinto, Biochem. Eng. J. 68 (2012) 85–90.
[28] G.L. Dotto, M.L.G. Vieira, V.M. Esquerdo, L.A.A. Pinto, Braz. J. Chem. Eng. 30 (2013) 13–21.
[29] N.F. Cardoso, E.C. Lima, B. Royer, M.V. Bach, G.L. Dotto, L.A.A. Pinto, T. Calvete, J. Hazard. Mater. 241–242 (2012) 146–153.
[30] J.A.V. Costa, M.G. Morais, Bioresour. Technol. 102 (2011) 2–9.
[31] M.G. Morais, C.C. Reichert, F. Dalcanton, A.J. Durante, L.F.F. Marins, J.A.V. Costa, Z. Naturforsch. 63 (2008) 144–150.
[32] J.A.V. Costa, L.M. Colla, P.F.D. Filho, Bioresour. Technol. 92 (2004) 237–241.
[33] E.G. Oliveira, G.S. Rosa, M.A. Moraes, L.A.A. Pinto, Bioresour. Technol. 100 (2009) 1297–1303.
[34] J. Bruce, R. Pecora, Dynamic Light Scattering: With Applications to Chemistry, Biology and Physics, Dover Publications, New York, 2000.
[35] R.H. Myers, D.C. Montgomery, Response Surface Methodology: Process and Product Optimization using Designed Experiments, John Wiley & Sons, New York, 2002.
[36] H. Freundlich, Z. Phys. Chem. A57 (1906) 358–471.
[37] I. Langmuir, J. Am. Chem. Soc. 40 (1918) 1361–1403.
[38] M.I. El-Khaiary, G.F. Malash, Hydrometallurgy 105 (2011) 314–320.
[39] J.S. Piccin, G.L. Dotto, L.A.A. Pinto, Braz. J. Chem. Eng. 28 (2011) 295–304.
[40] H. Bozdogan, Psychometrika 52 (1987) 345–370.
[41] Y. Liu, J. Chem. Eng. Data 54 (2009) 1981–1985.
[42] S.K. Milonjic, J. Serb. Chem. Soc. 72 (2007) 1363–1367.
[43] Y. Li, Q. Du, T. Liu, J. Sun, Y. Jiao, Y. Xia, L. Xia, Z. Wang, W. Zhang, K. Wang, H. Zhu, D. Wu, Mater. Res. Bull. 47 (2012) 1898–1904.
[44] J.C. Lazo-Cannata, A. Nieto-Márquez, A. Jacoby, A.L. Paredes Doig, A. Romero, M.R. Sun-Kou, J.L. Valverde, Sep. Purif. Technol. 80 (2011) 217–224.
[45] S. Mubarik, A. Saeed, Z. Mehmood, M. Iqbal, J. Taiwan Inst. Chem. Eng. 43 (2012) 926–933.
[46] C.H. Giles, T.H. MacEwan, S.N. Nakhwa, D. Smith, J. Chem. Soc. (1960) 3973–3993.
[47] A.H. Al-Muhtaseb, K.A. Ibrahim, A.B. Albadarin, O. Ali-khashman, G.M. Walker, M.N.M. Ahmad, Chem. Eng. J. 168 (2011) 691–699.
[48] R. Ocampo-Perez, R. Leyva-Ramos, J. Mendoza-Barron, R.M. Guerrero-Coronado, J. Colloid Interface Sci. 364 (2011) 195–204.
[49] A. Gundogdu, C. Duran, H.B. Senturk, M. Soylak, D. Ozdes, H. Serencam, M. Imamoglu, J. Chem. Eng. Data 57 (2012) 2733–2743.
[50] M. Zhong, Y. Wang, J. Yu, Y. Tian, G. Xu, Particuology 10 (2012) 35–41.
[51] C.L. Sun, C.S. Wang, J. Mol. Struct. 956 (2010) 38–43.
[52] B.V. Oepen, W. Kordel, W. Klein, Chemosphere 22 (1991) 285–304.